

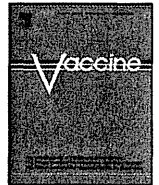
- 25 Cheever MA, Allison JP, Ferris AS *et al.* The prioritization of cancer antigens: a national cancer institute pilot project for the acceleration of translational research. *Clin Cancer Res* 2009; **15**: 5323–37.
- 26 Oka Y, Tsuboi A, Taguchi T *et al.* Induction of WT1 (Wilms' tumor gene)-specific cytotoxic T lymphocytes by WT1 peptide vaccine and the resultant cancer regression. *Proc Natl Acad Sci U S A* 2004; **101**: 13885–90.
- 27 Kawakami M, Oka Y, Tsuboi A *et al.* Clinical and immunologic responses to very low-dose vaccination with WT1 peptide (5 microg/body) in a patient with chronic myelomonocytic leukemia. *Int J Hematol* 2007; **85**: 426–9.
- 28 Kaida M, Morita-Hoshi Y, Soeda A *et al.* Phase 1 trial of Wilms tumor 1 (WT1) peptide vaccine and gemcitabine combination therapy in patients with advanced pancreatic or biliary tract cancer. *J Immunother* 2011; **34**: 92–9.
- 29 Rezvani K, Yong AS, Mielke S *et al.* Repeated PR1 and WT1 peptide vaccination in montanide-adjuvant fails to induce sustained high-avidity, epitope-specific CD8+ T cells in myeloid malignancies. *Haematologica* 2011; **96**: 432–40.
- 30 Tanaka-Harada Y, Kawakami M, Oka Y *et al.* Biased usage of BV gene families of T-cell receptors of WT1 (Wilms' tumor gene)-specific CD8+ T cells in patients with myeloid malignancies. *Cancer Sci* 2010; **101**: 594–600.
- 31 Nakatsuka S, Oji Y, Horiuchi T *et al.* Immunohistochemical detection of WT1 protein in a variety of cancer cells. *Mod Pathol* 2006; **19**: 804–14.
- 32 Valmori D, Scheibenbogen C, Dutoit V *et al.* Circulating tumor-reactive CD8(+) T cells in melanoma patients contain a CD45RA(+)CCR7(-) effector subset exerting *ex vivo* tumor-specific cytolytic activity. *Cancer Res* 2002; **62**: 1743–50.
- 33 Sallusto F, Lenig D, Förster R, Lipp M, Lanzavecchia A. Two subsets of memory T lymphocytes with distinct homing potentials and effector functions. *Nature* 1999; **401**: 708–12.
- 34 Valmori D, Dutoit V, Liénard D *et al.* Tetramer-guided analysis of TCR beta-chain usage reveals a large repertoire of melan-A-specific CD8+ T cells in melanoma patients. *J Immunol* 2000; **165**: 533–8.
- 35 Derré L, Bruyninx M, Baumgaertner P *et al.* *In vivo* persistence of codominant human CD8+ T cell clonotypes is not limited by replicative senescence or functional alteration. *J Immunol* 2007; **179**: 2368–79.
- 36 Wadia P, Rao D, Pradhan T, Pathak A, Chiplunkar S. Impaired lymphocyte responses and their restoration in oral cancer patients expressing distinct TCR variable region. *Cancer Invest* 2008; **26**: 471–80.
- 37 Dietrich PY, Walker PR, Quiquerez AL *et al.* Melanoma patients respond to a cytotoxic T lymphocyte-defined self-peptide with diverse and nonoverlapping T-cell receptor repertoires. *Cancer Res* 2001; **61**: 2047–54.
- 38 Willhauck M, Möhler T, Scheibenbogen C *et al.* T-cell receptor beta variable region diversity in melanoma metastases after interleukin 2-based immunotherapy. *Clin Cancer Res* 1996; **2**: 767–72.
- 39 Mandruzzato S, Rossi E, Bernardi F *et al.* Large and dissimilar repertoire of Melan-A/MART-1-specific CTL in metastatic lesions and blood of a melanoma patient. *J Immunol* 2002; **169**: 4017–24.
- 40 Zhou J, Dudley ME, Rosenberg SA, Robbins PF. Selective growth, *in vitro* and *in vivo*, of individual T cell clones from tumor-infiltrating lymphocytes obtained from patients with melanoma. *J Immunol* 2004; **173**: 7622–9.
- 41 Pospori C, Xue SA, Holler A *et al.* Specificity for the tumor-associated self-antigen WT1 drives the development of fully functional memory T cells in the absence of vaccination. *Blood* 2011; **117**: 6813–24.

Supporting Information

Additional Supporting Information may be found in the online version of this article:

Fig. S1. Statistical comparison of usage frequencies of T cell receptor β -chain variable region (TCR-BV) gene families in WT1₁₂₆ tetramer⁺ CD8⁺ T cells between naïve and effector memory fractions.

Please note: Wiley-Blackwell are not responsible for the content or functionality of any supporting materials supplied by the authors. Any queries (other than missing material) should be directed to the corresponding author for the article.



Enhanced tumor immunity of WT1 peptide vaccination by interferon- β administration[☆]

Hiroko Nakajima^a, Yoshihiro Oka^b, Akihiro Tsuboi^c, Naoya Tatsumi^d, Yumiko Yamamoto^e, Fumihiko Fujiki^a, Zheyu Li^e, Ayako Murao^b, Soyoko Morimoto^b, Naoki Hosen^e, Toshiaki Shirakata^{e,f}, Sumiyuki Nishida^c, Ichiro Kawase^b, Yoshitaka Isaka^g, Yusuke Oji^d, Haruo Sugiyama^{e,*}

^a Department of Cancer Immunology, Osaka University Graduate School of Medicine, Osaka, Japan

^b Department of Respiratory Medicine, Allergy and Rheumatic Diseases, Osaka University Graduate School of Medicine, Osaka, Japan

^c Department of Cancer Immunotherapy, Osaka University Graduate School of Medicine, Osaka, Japan

^d Department of Cancer Stem Cell Biology, Osaka University Graduate School of Medicine, Osaka, Japan

^e Department of Functional Diagnostic Science, Osaka University Graduate School of Medicine, 1-7, Yamada-Oka, Suita City, Osaka 565-0871, Japan

^f Department of Bioregulatory Medicine, Ehime University Graduate School of Medicine, Toon, Ehime, Japan

^g Department of Nephrology, Osaka University Graduate School of Medicine, Osaka, Japan

ARTICLE INFO

Article history:

Received 18 August 2011

Received in revised form

18 November 2011

Accepted 19 November 2011

Available online 29 November 2011

Key words:

WT1

IFN- β

Immunotherapy

Cancer vaccine

Adjuvant

ABSTRACT

To induce and activate tumor-associated antigen-specific cytotoxic T lymphocytes (CTLs) for cancer immunity, it is important not only to select potent CTL epitopes but also to combine them with appropriate immunopotentiating agents. Here we investigated whether tumor immunity induced by WT1 peptide vaccination could be enhanced by IFN- β . For the experimental group, C57BL/6 mice were twice pre-treated with WT1 peptide vaccine, implanted with WT1-expressing C1498 cells, and treated four times with WT1 peptide vaccine at one-week intervals. During the vaccination period, IFN- β was injected three times a week. Mice in control groups were treated with WT1 peptide alone, IFN- β alone, or PBS alone. The mice in the experimental group rejected tumor cells and survived significantly longer than mice in the control groups. The overall survival on day 75 was 40% for the mice treated with WT1 peptide + IFN- β , while it was 7, 7, and 0% for those treated with WT1 peptide alone, IFN- β alone or PBS alone, respectively. Induction of WT1-specific CTLs and enhancement of NK activity were detected in splenocytes from mice in the experimental group. Furthermore, administration of IFN- β enhanced expression of MHC class I molecules on the implanted tumor cells. In conclusion, our results showed that co-administration of WT1 peptide + IFN- β enhanced tumor immunity mainly through the induction of WT1-specific CTLs, enhancement of NK activity, and promotion of MHC class I expression on the tumor cells. WT1 peptide vaccination combined with IFN- β administration can thus be expected to enhance the clinical efficacy of WT1 immunotherapy.

© 2011 Elsevier Ltd. All rights reserved.

1. Introduction

Induction and activation of tumor-associated antigen (TAA)-specific cytotoxic T lymphocytes (CTLs) is essential for cancer immunotherapy. For this purpose, it is important to co-administer appropriate immunopotentiating agents, including adjuvants or cytokines, together with a TAA-derived peptide that serves as a CTL epitope, because injection of a CTL epitope alone cannot

sufficiently induce and activate the TAA-specific CTLs. Furthermore, if the co-administered agents not only help induction/activation of the CTLs but also activate other effector cells such as NK cells, this may further enhance anti-tumor responses.

The Wilms' tumor gene *WT1* was originally isolated as a gene responsible for Wilms' tumor, a pediatric renal cancer [1,2]. This gene encodes a zinc finger transcription factor involved in organ development, cell proliferation and differentiation, as well as apoptosis. The *WT1* gene product regulates the expression of various genes either positively or negatively, depending upon how it combines with other regulatory proteins in different types of cells. Although *WT1* was categorized at first as a tumor suppressor gene [3], we have proposed that the wild-type *WT1* gene plays an oncogenic rather than a tumor-suppressor gene function in leukemogenesis/tumorigenesis on the basis of the following

[☆] This study was supported in part by a Grant-in-Aid from the Ministry of Education, Culture, Sports, Science and Technology and the Ministry of Health, Labor, and Welfare, Japan.

* Corresponding author. Tel.: +81 6 6879 2593; fax: +81 6 6879 2593.

E-mail address: sugiyama@sahs.med.osaka-u.ac.jp (H. Sugiyama).

–7. During the same period, 50,000 units of murine IFN- β was intraperitoneally (i.p.) injected three times per week. On day 0, mice were subcutaneously (s.c.) implanted with 3×10^5 mWT1-C1498 cells in 100 μ l of PBS, followed by abdominal i.d. injection of 100 μ g WT1 peptide emulsified with IFA on days 1, 8, 15, and 22. In addition, 50,000 units of murine IFN- β was also injected i.p. three times per week until day 26. Mice in control groups were vaccinated with WT1 peptide + IFA + PBS (WT1 peptide alone group); PBS + IFA + IFN- β (IFN- β alone group); and PBS + IFA + PBS (non-treated group). Tumor growth was monitored by measuring the longest diameter of the palpable mass.

For the assessment of immunological effector cells, we performed *in vivo* experiments independently from those for the assessment of survival. Splenocytes and bone marrow cells from mice immunized as shown in Fig. 1 were recovered on day 30 (8 days after the last vaccination) and used for ^{51}Cr release cytotoxicity assay (CTL and NK activities) and colony assay, respectively. Furthermore, the resected tumors were used for analysis of MHC class I expression.

2.5. ^{51}Cr release cytotoxicity assay and mice treatment schedule for the assay

Splenocytes were stimulated with the 5 μ g/ml WT1 peptide and cultured in complete medium containing 10% heat-inactivated FCS, 45% RPMI1640 medium, 45% AIM-V medium, 1 \times non-essential amino acid (Gibco), 25 ng/ml 2-mercaptoethanol, 50 IU/ml penicillin and 50 μ g/ml streptomycin. Two and four days later, recombinant interleukin-2 (rIL-2; kindly donated by Shionogi Biomedical Laboratories, Osaka, Japan) was added to the culture at a concentration of 20 IU/ml. After six days of culture, a ^{51}Cr release cytotoxicity assay was performed against WT1 peptide-pulsed or -unpulsed RMA cells for WT1-specific CTL activity, and against YAC-1 cells for NK cell activity, as described previously [24]. Target cells (1×10^4 cells) labeled with ^{51}Cr were added to wells containing varying numbers of effector cells in 96-well plates. After 4 h of incubation at 37 $^\circ\text{C}$, cell lysates were centrifuged and 100 μ l of the supernatant was collected and measured for radioactivity. The percentage of specific lysis (% specific lysis) was calculated as follows: percentage of specific lysis = (cpm of experimental release – cpm of spontaneous release) / (cpm of maximal release – cpm of spontaneous release) \times 100. Radioactivity of the supernatant, either of the target cell cultures without effector cells, or of the target cells that were completely lysed by the treatment with 1% Triton X-100 was used for spontaneous and maximal release, respectively.

2.6. Analysis of MHC class I expression

Tumors were resected from the tumor-bearing mice on day 30, and tumor cell suspensions were prepared with the tissues in the center of the tumor mass. The resected tissues contained only tumor mass with the naked eye. The cells were stained with FITC-conjugated anti-mouse H-2D^b monoclonal antibody (KH-95, BD Biosciences, Franklin Lakes, NJ, USA) and analyzed with the FACSsort (BD). Live cells were determined by means of FSC and SSC gating.

2.7. Colony assay

For CFU-GM (colony-forming-unit granulocyte-macrophage) assay, bone marrow cells were recovered from mice on day 30, plated at 1×10^4 cells/plate in methylcellulose medium containing 10 ng/ml IL-3, 10 ng/ml IL-6, 50 ng/ml SCF, and 3 U/ml erythropoietin (EPO) (Methocult M3434; Stem Cell Technologies, Vancouver, BC, Canada), and cultured at 37 $^\circ\text{C}$ in a humidified incubator under 5% CO₂. Colonies with more than 50 cells were counted on days 8 and 12.

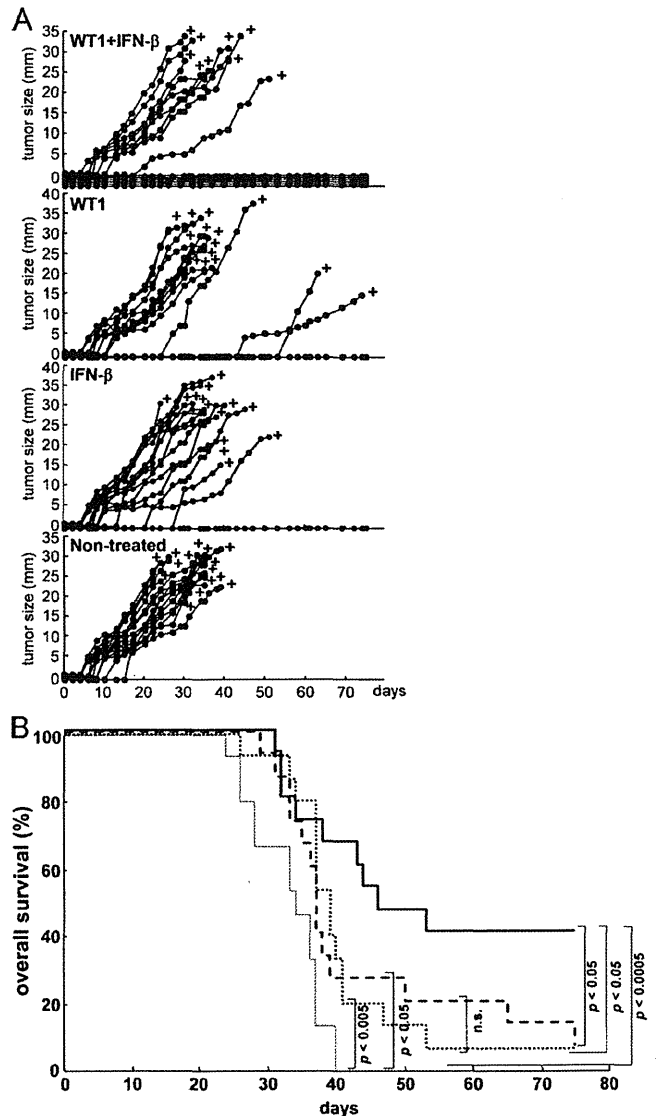


Fig. 2. Effect of WT1 peptide vaccination combined with IFN- β administration on rejection of implanted tumor cells. (A) Time course of size of tumors developed in individual mice of the four groups. Tumor sizes represent the longest diameters. (B) Overall survival curves of the four groups. Solid black, broken, dotted, and solid gray lines represent overall survival curves of mice treated with WT1 peptide vaccine + IFN- β , WT1 peptide vaccine alone, IFN- β alone, and non-treated mice, respectively.

2.8. *In vivo* CD8⁺ T and NK cell depletion experiments

Mice were implanted with 3×10^5 mWT1-C1498 cells and treated with WT1 peptide vaccine + IFN- β as shown Fig. 1. The WT1- and IFN- β - treated mice were injected with PBS or 200 μ g of anti-CD8 and/or 200 μ g of anti-NK mAbs on days –15, –8, –1, 4, 7, 11, 14, 18, 21 and 25 [35,41].

2.9. Statistical analysis

Significant differences in overall survivals among experimental groups were evaluated with the Logrank test. The Student's *t*-test was used to calculate the differences in the expression levels of H-2D^b on tumor cells in mice among experimental groups.

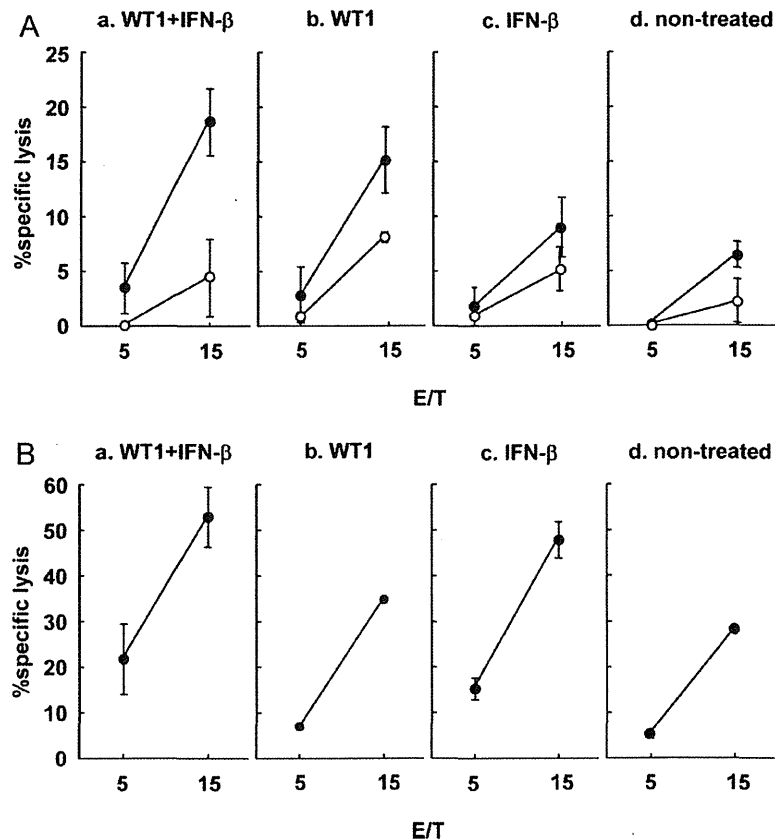


Fig. 3. Induction of WT1-specific CTLs and enhancement of NK activity by treatment with WT1 peptide vaccine + IFN- β . Eight days after the last vaccination, splenocytes from the mice in each group were stimulated *in vitro* with WT1 peptide-pulsed synergistic splenocytes. WT1-specific CTL and NK cell activities were assayed in triplicate as cytotoxic activities against WT1 peptide-pulsed, -unpulsed RMAS or YAC-1 cells, respectively, at the indicated E/T ratio. (A) WT1-specific CTL activity. Closed and open circles represent cytotoxic activities against WT1 peptide-pulsed or -unpulsed RMAS, respectively. (B) NK activity. NK activity is shown as cytotoxic activities against YAC-1 cells. Bars indicate standard errors.

3. Results

3.1. IFN- β promotes efficacy of WT1 peptide vaccination

To investigate whether IFN- β promoted tumor cell rejection by WT1 peptide vaccination, mice were twice immunized with Montanide ISA51-emulsified WT1 peptide with or without IFN- β administration before transplantation of WT1-expressing tumor cells (mWT1-C1498) and then repeatedly WT1-immunized, followed by assessment of the tumor growth and their survival (Fig. 1). Optimization of cell number and determination of the observation period are described in Section 2.

Nine of the 15 mice treated with WT1 peptide vaccine + IFN- β developed tumors and died, while the remaining 6 mice were alive without tumors on day 75 (Fig. 2A). In contrast, 14 of the 15 mice treated with WT1 peptide vaccine alone, 14 of the 15 mice treated with IFN- β alone and all of the 15 non-treated mice had died of tumor growth by day 75. Overall survival rates on day 75 were 40% for mice treated with WT1 peptide vaccine + IFN- β , but 7, 7 and 0% for mice treated with WT1 peptide vaccine alone or IFN- β alone or for non-treated mice, respectively. The overall survival rates of mice treated with WT1 peptide vaccine + IFN- β were significantly higher than those of the other three groups (WT1 peptide vaccine + IFN- β versus WT1 peptide vaccine alone, IFN- β alone or non-treated: $p < 0.05$, $p < 0.05$, and $p < 0.0005$, respectively). The overall survival rates of mice treated with WT1 peptide vaccine alone or IFN- β alone were significantly higher than those of non-treated (WT1 peptide vaccine alone versus non-treated, IFN- β alone versus non-treated:

$p < 0.05$ and $p < 0.005$, respectively). There was no significant difference in survival rate between WT1 peptide vaccine alone and IFN- β alone (Fig. 2B).

3.2. WT1 peptide vaccine + IFN- β enhances induction of WT1-specific CTLs and activates NK cell activity

In order to analyze immune responses, tumor-bearing mice treated with WT1 peptide vaccine + IFN- β as shown in Fig. 1 were sacrificed on day 30. The splenocytes of each mouse were stimulated *in vitro* with WT1 peptide and assayed for WT1 peptide-specific CTL activity against WT1 peptide-pulsed and -unpulsed RMAS cells and for NK activity against YAC-1 cells. Representative data are shown in Fig. 3. Splenocytes from mice treated with WT1 peptide vaccine + IFN- β showed the strongest WT1 peptide-specific cytotoxic activity while splenocytes from non-treated mice showed the weakest activity. WT1-specific cytotoxic activity was in the following order: WT1 peptide vaccine + IFN- β > WT1 peptide vaccine alone > IFN- β alone > non-treated. These findings convincingly showed that WT1-specific CTL activity was higher in the two groups with WT1 peptide vaccine than in the two groups without it. It appeared that the WT1-specific CTL activities in splenocytes from IFN- β -treated or non-treated mice were endogenously induced as a result of immunological stimulation by WT1-expressing tumor cells implanted.

Next, NK cell activity was examined (Fig. 3B). Mice of all four groups were sacrificed on day 30 and their splenocytes were analyzed for their NK cell activity. NK cell activity was higher in both

WT1 peptide vaccine + IFN- β and IFN- β alone groups. These results suggested that NK activity was endogenously induced in WT1-expressing tumor-bearing mice and that this activity was enhanced by administration of IFN- β , which is a potent enhancer of NK activity.

Taken together, these results indicated that the strongest rejection of implanted tumor cells in the mice treated with WT1 peptide vaccine + IFN- β resulted from the generation of the highest levels of both WT1-specific CTLs and NK cells.

3.3. WT1 specific CTLs and NK cells play crucial roles in the treatment by WT1 peptide vaccine + IFN- β

To confirm that WT1-specific CTLs and NK cells played crucial roles in the tumor rejection, *in vivo* depletion of CD8⁺ T and/or NK cells was performed. Mice that were implanted with mWT1-C1498 cells and vaccinated with WT1 peptide vaccine + IFN- β as shown in Fig. 1 were treated with both or either of anti-CD8 and anti-NK mAbs.

Two of five mAb-non-treated mice developed tumors and died, while the remaining three survived without development of tumors. In contrast, all of the mice that were treated with both or either of anti-CD8 and anti-NK mAbs and vaccination-non-treated mice died of tumor development. It should be noted that appearance of tumors in mice treated with both or either anti-CD8 and anti-NK mAbs was earlier than that in mAb-non-treated mice (Fig. 4).

These results strongly indicated that both WT1-specific CD8⁺ CTLs and NK cells played crucial roles in the rejection of tumor cells.

3.4. Enhancement of MHC class I (H-2D^b) expression on transplanted tumor cells by the administration of IFN- β

Since WT1 (Db126) peptide is produced from WT1 protein through processing in tumor cells and presents on the cell surface in association with MHC class I (H-2D^b) [29,32], H-2D^b expression levels of target cells are thought to exert a major influence on the susceptibility of the cells to attack by vaccination-induced WT1 (Db126)-specific CTLs. For this reason, the H-2D^b expression levels on the transplanted tumor cells (WT1-expressing C1498 cells) were examined. Tumor-bearing mice were sacrificed 30 days after tumor cell implantation, the tumors were resected, and the tumor cells were stained with anti-H-2D^b antibody (Fig. 5). The expression levels of H-2D^b on tumor cells was significantly higher in mice treated with WT1 peptide vaccine + IFN- β or IFN- β alone than in those treated with WT1 peptide vaccine alone or non-treated mice ($p < 0.05$) (Fig. 5B). These results indicated that IFN- β administration enhanced the expression of H-2D^b on tumor cells, which should make tumor cells more susceptible to attack by WT1-specific CTLs.

3.5. No inhibition of colony-forming ability of bone marrow cells from mice immunized with WT1 peptide vaccine + IFN- β

WT1 is expressed in some tissues of normal adult mice, including hematopoietic stem/progenitor cells, podocytes of kidney glomeruli, gonads and mesothelial structures. To evaluate the risk of induction of autoimmunity by immunization with WT1 peptide vaccine + IFN- β , the colony-forming ability of bone marrow cells, as shown by the numbers of CFU-GM colonies, were examined. No differences in numbers of CFU-GM colonies were found among the five groups (WT1 peptide vaccine + IFN- β , WT1 peptide vaccine alone, IFN- β alone, tumor-bearing non-treated, and non-tumor-bearing non-treated) (Fig. 6). These results showed that induced

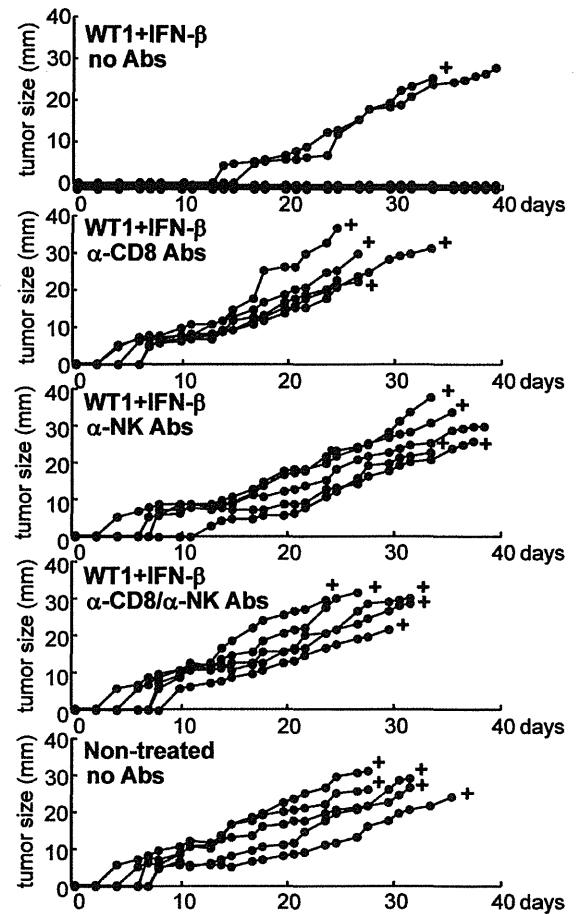


Fig. 4. Cancellation of tumor rejection by WT1 peptide vaccine + IFN- β by the administration of anti-CD8 and/or anti-NK mAbs. Mice were implanted with 3×10^5 mWT1-C1498 cells and treated with WT1 peptide vaccine + IFN- β as shown in Fig. 1. The WT1- and IFN- β -treated mice were injected with PBS or 200 μ g of anti-CD8 and/or 200 μ g of anti-NK mAbs on days -15, -8, -1, 4, 7, 11, 14, 18, 21 and 25. Time course of size of tumors developed in individual mice from the five groups. Tumor sizes represent the longest diameters.

WT1-specific CTLs did not recognize normal cells that physiologically expressed WT1.

4. Discussion

In the study presented here, we demonstrated that co-treatment with WT1 peptide vaccine (Db126; CTL epitope) + IFN- β enhanced rejection of WT1-expressing tumor cells in a mouse model. Enhanced induction of WT1-specific CTLs and NK cell activity was considered to be largely responsible for the successful rejection of the implanted tumor cells. The important roles of WT1-specific CD8⁺ T cells and NK cells in the tumor rejection were confirmed by depletion experiments using anti-CD8 and/or anti-NK mAbs.

The most likely mechanism for the induction of the strongest WT1-specific cytotoxic activity in mice treated with WT1 peptide vaccine + IFN- β is the following: IFN- β activates NK cells [30,42,45], which generate IFN- γ , which in turn activates DCs and T cells [42–44]. Furthermore, IFN- β can also activate T cells directly [30]. These conditions lead to a more efficient induction of WT1-specific CTLs by the WT1 peptide vaccine. The WT1 peptide-specific cytotoxic activity observed in tumor-bearing non-treated mice may be due to the spontaneous induction of WT1-specific CTLs as a result of immune stimulation by implanted WT1-expressing tumors. Enhancement of NK cell function induced by *in vivo*

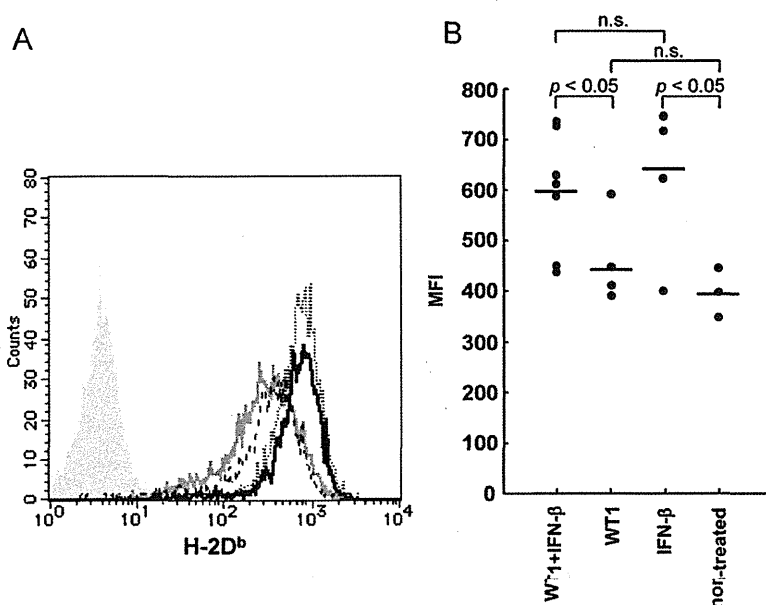


Fig. 5. IFN- β enhanced MHC class I (H-2D^b) expression of tumor cells *in vivo*. (A) H-2D^b expression levels of tumor cells recovered from mice. Solid black, broken, dotted, and solid gray lines represent the expression levels of tumor cells from mice treated with WT1 peptide vaccine + IFN- β , WT1 peptide vaccine alone, or IFN- β alone, and non-treated mice, respectively. (B) The mean fluorescence intensity (MFI) of H-2D^b expression of tumor cells from mice.

administration of IFN- β contributed to a high rejection rate of tumors in the present experiment system. However, the exact mechanism of the enhancement was not addressed in this study, while a series of investigations regarding the effect of IFN- β on NK cells were reported, including that IFN- β upregulated TRAIL on NK cells [45] and enhanced production of IFN- γ from NK cells. Besides NK cells, NKT cells might also have important roles in enhancement of tumor rejection in the present experiment system, considering that it was reported that IFN- β enhanced up-regulation of CD1d on DCs, which leads to NKT cell activation [46]. Further studies are needed to address the mechanism of enhancement of NK and NKT cell function by IFN- β in the context of tumor immunity.

At least two merits of IFN- β administration could be confirmed. One was that, as shown in Fig. 3B, greater enhancement of NK cell activity was observed in mice treated with WT1 peptide vaccine + IFN- β or with IFN- β alone than in the other two groups. This indicates that IFN- β activated NK cells *in vivo*, and that the enhanced NK activity contributed to eradication of MHC class

I-negative tumor cells or those with low MHC class I expression. Another merit was that MHC class I expression on the WT1-C1498 leukemia cells was enhanced. WT1 peptides were generated through intracellular processing of the WT1 protein in tumor cells and presented on the surface of these cells in association with MHC class I molecules, followed by the recognition of the WT1 peptide/MHC class I complex by WT1-specific CTLs. Consistent with previously reported findings [28,29], MHC-class I expression on the WT1-C1498 leukemia cells was enhanced in mice treated with WT1 peptide vaccine + IFN- β or IFN- β alone. Higher expression of MHC class I molecules contributes the recognition and attack by CTLs [29]. It is possible that in mice treated with WT1 peptide vaccine + IFN- β MHC class I expression on the WT1-C1498 leukemia cells was enhanced, resulting in a heightened vulnerability to attack by WT1-specific CTLs. Taken together, it seems likely that target cells (mWT1-C1498 cells), of which the MHC class I expression was enhanced by IFN- β , were efficiently killed by WT1-specific CTLs, while the remaining target cells with negative or low MHC class I expression were efficiently killed by NK cells whose activity was enhanced by IFN- β . IFN- α is another type I IFN and has the similar structure and function to IFN- β [31–36,45,47]. Furthermore, both IFN- α and IFN- β were approved for human use [30,37–40,48]. Therefore, it would be interesting to examine, using this experiment system, whether IFN- α , as well as IFN- β , is effective in the context of a combined use with WT1 peptide vaccine for the treatment of malignancies.

Other functions of IFN- β in tumor rejection enhancement, that is, non-immunological mechanisms such as direct anti-tumor and anti-angiogenesis effect [32–34] may also have contributed to such rejection.

Although WT1 is physiologically expressed in some type of normal cells, including hematopoietic stem/progenitor cells and kidney glomeruli, WT1 vaccination combined with IFN- β treatment did not diminish the GM colony-forming ability of BM cells (Fig. 6), which is in agreement with previous reports [25,27]. These findings indicate that WT1-specific CTLs did not recognize normal cells that physiologically expressed WT1. The reason for this lack of recognition appears to be that WT1-specific CTLs can

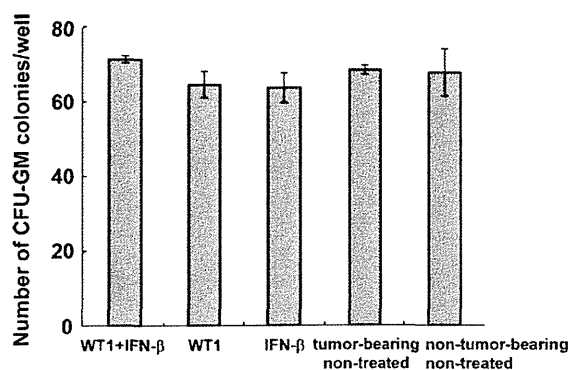


Fig. 6. No inhibition of colony-forming ability of bone marrow cells from mice immunized with WT1 peptide vaccine + IFN- β . Numbers of colonies generated by CFU-GM (colony-forming-unit granulocyte-macrophage) from mouse bone marrow cells on day 30. Values represent the means of the results from four mice in each group. Bars indicate standard errors.

discriminate only between WT1-expressing tumor cells and physiologically WT1-expressing normal cells, resulting in the selective killing of tumor cells with no damage to normal tissues. These results suggested that the mechanisms involved in processing of WT1 protein and/or presentation of WT1 peptide might be different between tumor and normal cells, resulting in no or weak presentation of the WT1 peptide on the cell surface of normal cells. Further studies to address this issue are clearly warranted.

Immunopotentiating agents play a key role in the success of cancer immunotherapy, because injection of CTL epitope peptide alone cannot sufficiently induce and activate the TAA-specific CTLs. Co-administration of CTL epitope peptides and immunopotentiating agents proved to be effective for induction and activation of the CTLs and/or activation of other effector cells such as NK cells. We previously reported that the WT1 peptide vaccine combined with *M. bovis* bacillus Calmette-Guérin cell wall skeleton (BCG-CWS), which activates DCs through TLRs 2 and 4, had a synergistic effect on tumor rejection in mice [27]. In the current study, we could demonstrate the immunopotentiating activities of IFN- β leading to the enhancement of WT1-specific CTLs, NK cells, and MHC class I expression. It is anticipated that WT1 peptide vaccination combined with both IFN- β and BCG-CWS will be more effective for tumor rejection. The combination of CTL epitope vaccine with some immunopotentiating agents with various mechanisms for enhancement of anti-tumor immunity can be expected to become part of effective strategies for the cancer immunotherapy. Clinical trials of WT1 peptide cancer vaccine have already been started, and WT1 peptide vaccination was shown to have good potential for the treatment of cancer [14–17,49–54]. So far, we have performed immunization using WT1 peptide with Montanide ISA 51 adjuvant, and another group used KLH and GM-CSF [55]. Since the safety and toxicity of IFN- β have been confirmed to a considerable extent [37–40], WT1 peptide vaccination combined with IFN- β should be ready for use in the clinical settings in the near future.

Acknowledgement

We would like to thank Ms. Sachie Mamitsuka-Watanabe for preparation of this manuscript.

References

- [1] Call KM, Glaser T, Ito CY, Buckler AJ, Pelletier J, Haber DA, et al. Isolation and characterization of a zinc finger polypeptide gene at the human chromosome 11 Wilms' tumor locus. *Cell* 1990;60:509–20.
- [2] Gessler M, Poustka A, Cavenee W, Nevel RL, Orkin SH, Bruns GAP. Homozygous deletion in Wilms tumors of a zinc-finger gene identified by chromosome jumping. *Nature* 1990;343:774–8.
- [3] Menke AL, Van der Eb AJ, Jochemsen AG. The Wilms' tumor 1 gene: oncogene or tumor suppressor gene. *Int Rev Cytol* 1998;181:151–212.
- [4] Inoue K, Sugiyama H, Ogawa H, Nakagawa M, Yamagami T, Miwa H, et al. WT1 as a new prognostic factor and a new marker for the detection of minimal residual disease in acute leukemia. *Blood* 1994;84:3071–9.
- [5] Inoue K, Ogawa H, Sonoda Y, Kimura T, Sakabe H, Oka Y, et al. Aberrant overexpression of the Wilms' tumor gene (WT1) in human leukemia. *Blood* 1997;89:1405–12.
- [6] Briegar J, Weidmann E, Fenchel K, Mitrou PS, Hoelzer D, Bergmann L. The expression of the Wilms' tumor gene in acute myelocytic leukemias as a possible marker for leukemic blast cells. *Leukemia* 1994;8:2138–43.
- [7] Miwa H, Beran M, Saunders GF. Expression of the Wilms' tumor gene (WT1) in human leukemias. *Leukemia* 1992;6:405–9.
- [8] Menssen HD, Renkl HJ, Rodeck U, Maurer J, Notter M, Schwartz S, et al. Presence of Wilms' tumor gene (WT1) transcripts and the WT1 nuclear protein in the majority of human acute leukemias. *Leukemia* 1995;9:1060–7.
- [9] Oji Y, Ogawa H, Tamaki H, Oka Y, Tsuboi A, Kim EH, et al. Expression of the Wilms' tumor gene WT1 in solid tumors and its involvement in tumor cell growth. *Jpn J Cancer Res* 1999;90:194–204.
- [10] Oji Y, Miyoshi S, Maeda H, Hayashi S, Tamaki H, Nakatsuka S, et al. Overexpression of the Wilms' tumor gene WT1 in de novo lung cancers. *Int J Cancer* 2002;100:297–303.
- [11] Loeb DM, Evron E, Patel CB, Sharma PM, Niranjani B, Buluwela L, et al. Wilms' tumor suppressor gene (WT1) is expressed in primary breast tumors despite tumor-specific promotor methylation. *Cancer Res* 2001;61:921–5.
- [12] Oji Y, Yamamoto H, Nomura M, Nakano Y, Ikeba A, Nakatsuka S, et al. Overexpression of the Wilms' tumor gene WT1 in colorectal adenocarcinoma. *Cancer Sci* 2003;94:712–7.
- [13] Oji Y, Suzuki T, Nakano Y, Maruno M, Nakatsuka S, Jongeom T, et al. Overexpression of the Wilms' tumor gene WT1 in primary astrocytic tumors. *Cancer Sci* 2004;95:822–7.
- [14] Sugiyama H. Cancer immunotherapy targeting WT1 protein. *Int J Hematol* 2002;76:127–32.
- [15] Sugiyama H. Cancer immunotherapy targeting Wilms' tumor gene WT1 product. *Expert Rev Vaccines* 2005;4:503–12.
- [16] Oka Y, Tsuboi A, Kawakami M, Elisseeva OA, Nakajima H, Udaka K, et al. Development of WT1 peptide cancer vaccine against hematopoietic malignancies and solid cancers. *Curr Med Chem* 2006;13:2345–52.
- [17] Oka Y, Tsuboi A, Elisseeva OA, Nakajima H, Fujiki F, Kawakami M, et al. WT1 peptide cancer vaccine for patients with hematopoietic malignancies and solid cancers. *ScientificWorldJournal* 2007;29:649–65.
- [18] Yamagami T, Sugiyama H, Inoue K, Ogawa H, Tatekawa T, Hirata M, et al. Growth inhibition of human leukemic cells by WT1 (Wilms tumor gene) antisense oligonucleotides: implications for the involvement of WT1 in leukemogenesis. *Blood* 1996;87:2878–84.
- [19] Inoue K, Tamaki H, Ogawa H, Oka Y, Soma T, Tatekawa T, et al. Wilms' tumor gene (WT1) competes with differentiation-inducing signal in hematopoietic progenitor cells. *Blood* 1998;91:2969–76.
- [20] Tsuboi A, Oka Y, Ogawa H, Elisseeva OA, Tamaki H, Oji Y, et al. Constitutive expression of the Wilms' tumor gene WT1 inhibits the differentiation of myeloid progenitor cells but promotes their proliferation in response to granulocyte-colony stimulating factor (G-CSF). *Leuk Res* 1999;23:499–505.
- [21] Oka Y, Elisseeva OA, Tsuboi A, Ogawa H, Tamaki H, Li H, et al. Human cytotoxic T-lymphocyte response specific for peptides of the wild-type Wilms' tumor gene (WT1) product. *Immunogenetics* 2000;51:99–107.
- [22] Gao L, Bellantuono I, Elsässer A, Marley SB, Gordon MY, Goldman JM, et al. Selective elimination of leukemic CD34⁺ progenitor cells by cytotoxic T lymphocytes specific for WT1. *Blood* 2000;95:2198–203.
- [23] Ohnishi H, Yasukawa M, Fujita S. HLA class I-restricted lysis of leukemia cells by a CD8⁺ cytotoxic T-lymphocyte clone specific for WT1 peptide. *Blood* 2000;95:286–93.
- [24] Oka Y, Udaka K, Tsuboi A, Elisseeva OA, Ogawa H, Aozasa K, et al. Cancer immunotherapy targeting Wilms' tumor gene WT1 product. *J Immunol* 2000;164:1873–80.
- [25] Tsuboi A, Oka Y, Ogawa H, Elisseeva OA, Li H, Kawasaki K, et al. Cytotoxic T-lymphocyte responses elicited to Wilms' tumor gene WT1 product by DNA vaccination. *J Clin Immunol* 2000;20:195–202.
- [26] Yasumoto K, Manabe H, Yanagawa E, Nagano N, Ueda H, Hirota N, et al. Non-specific adjuvant immunotherapy of lung cancer with cell wall skeleton of *Mycobacterium bovis* Bacillus Calmette-Guérin. *Cancer Res* 1979;39:3262–7.
- [27] Nakajima H, Kawasaki K, Oka Y, Tsuboi A, Kawakami M, Ikegami K, et al. WT1 peptide vaccination combined with BCG-CWS is more efficient for tumor eradication than WT1 peptide vaccination alone. *Cancer Immunol Immunother* 2004;53:617–24.
- [28] Dhib-Jalbut SS, Cowan EP. Direct evidence that interferon- β mediates enhanced HLA-Class I expression in measles virus-infected cells. *J Immunol* 1993;151:6248–58.
- [29] Dezfouli S, Hatzinisiriou I, Ralph SJ. Enhancing CTL responses to melanoma cell vaccines in vivo: synergistic increases obtained using IFN- γ primed and IFN- β treated B7-1⁺ B16-F10 melanoma cells. *Immunol Cell Biol* 2003;81:459–71.
- [30] Kirkwood JM, Richards T, Zarour HM, Sosman J, Ernstoff M, Whiteside TL, et al. Immunomodulatory effects of high-dose and low-dose interferon $\alpha 2b$ in patients with high-risk resected melanoma: the E2690 laboratory corollary of intergroup adjuvant trial E1690. *Cancer* 2002;95:1101–12.
- [31] Kayagaki N, Yamaguchi N, Nakayama M, Eto H, Okumura K, Yagita H. Type I interferons (IFNs) regulate tumor necrosis factor-related apoptosis-inducing ligand (TRAIL) expression on human T cells: a novel mechanism for the antitumor effects of type I IFNs. *J Exp Med* 1999;189:1451–60.
- [32] Tanabe T, Kominsky SL, Subramaniam PS, Johnson HM, Torres BA. Inhibition of the glioblastoma cell cycle by type I IFNs occurs at both the G1 and S phases and correlates with the upregulation of p21(WAF1/CIP1). *J Neurooncol* 2000;48:225–32.
- [33] Chen Q, Gong B, Mahmoud-Ahmed AS, Zhou A, Hsi ED, Hussein M, et al. Apo2L/TRAIL and Bcl-2-related proteins regulate type I interferon-induced apoptosis in multiple myeloma. *Blood* 2001;98:2183–92.
- [34] Streck CJ, Zhang Y, Miyamoto R, Zhou J, Ng CY, Nathwani AC, et al. Restriction of neuroblastoma angiogenesis and growth by interferon- α/β . *Surgery* 2004;136:183–9.
- [35] Wakita D, Chamoto K, Zhang Y, Narita Y, Noguchi D, Ohnishi H, et al. An indispensable role of type-I IFNs for inducing CTL-mediated complete eradication of established tumor tissue by CpG-liposome co-encapsulated with model tumor antigen. *Int Immunol* 2006;18:425–34.
- [36] Gehring S, Gregory SH, Kuzushita N, Wands JR. Type 1 interferon augments DNA-based vaccination against hepatitis C virus core protein. *J Med Virol* 2005;75:249–57.
- [37] Mani S, Todd M, Poo WJ. Recombinant beta-interferon in the treatment of patients with metastatic renal cell carcinoma. *Am J Clin Oncol* 1996;19:187–9.
- [38] Fine HA, Wen PY, Robertson M, O'Neill A, Kowal J, Loeffler JS, et al. A phase I trial of a new recombinant human beta-interferon (BG9015) for the treatment of patients with recurrent gliomas. *Clin Cancer Res* 1997;3:381–7.

- [39] Beppu T, Kamada K, Nakamura R, Oikawa H, Takeda M, Fukuda T, et al. A phase II study of radiotherapy after hyperbaric oxygenation combined with interferon-beta and nimustine hydrochloride to treat supratentorial malignant gliomas. *J Neurooncol* 2003;61:161–70.
- [40] Watanabe T, Katayama Y, Yoshino A, Fukaya C, Yamamoto T. Human interferon beta, nimustine hydrochloride, and radiation therapy in the treatment of newly diagnosed malignant astrocytomas. *J Neurooncol* 2005;72:57–62.
- [41] Yamaguchi S, Tatsumi T, Takehara T, Sakamori R, Uemura A, Mizushima T, et al. Immunotherapy of murine colon cancer using receptor tyrosine kinase EphA2-derived peptide-pulsed dendritic cell vaccines. *Cancer* 2007;110:1469–77.
- [42] Degli-Esposti MA, Smyth MJ. Close encounters of different kinds: dendritic cells and NK cells take centre stage. *Nat Rev Immunol* 2005;5:112–24.
- [43] Fedele G, Frasca L, Palazzo R, Ferrero E, Malavasi F, Ausiello CM. CD38 is expressed on human mature monocyte-derived dendritic cells and is functionally involved in CD83 expression and IL-12 induction. *Eur J Immunol* 2004;34:1342–50.
- [44] He T, Tang C, Xu S, Moyana T, Xiang J. Interferon gamma stimulates cellular maturation of dendritic cell line DC2.4 leading to induction of efficient cytotoxic T cell responses and antitumor immunity. *Cell Mol Immunol* 2007;4:105–11.
- [45] Sato K, Hida S, Takayanagi H, Yokochi T, Kayagaki N, Takeda K, et al. Antiviral response by natural killer cells through TRAIL gene induction by IFN- α/β . *Eur J Immunol* 2001;31:3138–46.
- [46] Raghuraman G, Geng Y, Wang CR. IFN- β -mediated up-regulation of CD1d in bacteria-infected APCs. *J Immunol* 2006;177:7841–8.
- [47] Gresser I. The antitumor effects of interferon: a personal history. *Biochimie* 2007;89:723–8.
- [48] Anguille S, Lion E, Willems Y, Van Tendeloo VF, Berneman ZN, Smits EL. Interferon- α in acute myeloid leukemia: an old drug revisited. *Leukemia* 2011;25:739–48.
- [49] Oka Y, Tsuboi A, Murakami M, Hirai M, Tominaga N, Nakajima H, et al. Wilms tumor gene peptide-based immunotherapy for patients with overt leukemia from myelodysplastic syndrome (MDS) or MDS with myelofibrosis. *Int J Hematol* 2003;78:56–61.
- [50] Tsuboi A, Oka Y, Osaki T, Kumagai T, Tachibana I, Hayashi S, et al. WT1 peptide-based immunotherapy for patients with lung cancer: report of two cases. *Microbiol Immunol* 2004;48:175–84.
- [51] Oka Y, Tsuboi A, Taguchi T, Osaki T, Kyo T, Nakajima H, et al. Induction of WT1 (Wilms' tumor gene)-specific cytotoxic T lymphocytes by WT1 peptide vaccine and the resultant cancer regression. *Proc Natl Acad Sci USA* 2004;101:13885–90.
- [52] Morita S, Oka Y, Tsuboi A, Kawakami M, Maruno M, Izumoto S, et al. A phase I/II trial of a WT1 (Wilms' tumor gene) peptide vaccine in patients with solid malignancy: safety assessment based on the phase I data. *Jpn J Clin Oncol* 2006;36:231–6.
- [53] Kawakami M, Oka Y, Tsuboi A, Harada Y, Elisseeva OA, Furukawa Y, et al. Clinical and immunologic responses to very low-dose vaccination with WT1 peptide (5 $\mu\text{g}/\text{body}$) in a patient with chronic myelomonocytic leukemia. *Int J Hematol* 2007;85:426–9.
- [54] Iiyama T, Udaka K, Takeda S, Takeuchi T, Adachi YC, Ohtsuki Y, et al. WT1 (Wilms' tumor 1) peptide immunotherapy for renal cell carcinoma. *Microbiol Immunol* 2007;51:519–30.
- [55] Mailänder V, Scheibenbogen C, Thiel E, Letsch A, Blau IW, Keilholz U. Complete remission in a patient with recurrent acute myeloid leukemia induced by vaccination with WT1 peptide in the absence of hematological or renal toxicity. *Leukemia* 2004;18:165–6.

Use of ^{11}C -methionine PET parametric response map for monitoring WT1 immunotherapy response in recurrent malignant glioma

Clinical article

YASUYOSHI CHIBA, M.D., PH.D.,¹ MANABU KINOSHITA, M.D., PH.D.,¹
 YOSHIKO OKITA, M.D., PH.D.,¹ AKIHIRO TSUBOI, M.D., PH.D.,²
 KAYAKO ISOHASHI, M.D., PH.D.,³ NAOKI KAGAWA, M.D., PH.D.,¹
 YASUNORI FUJIMOTO, M.D., PH.D.,¹ YUSUKE OJI, M.D., PH.D.,⁴
 YOSHIHIRO OKA, M.D., PH.D.,⁵ EKU SHIMOSEGAWA, M.D., PH.D.,³ SATOSHI MORITA, PH.D.,⁶
 JUN HATAZAWA, M.D., PH.D.,³ HARUO SUGIYAMA, M.D., PH.D.,⁷
 NAOYA HASHIMOTO, M.D., PH.D.,¹ AND TOSHIKI YOSHIMINE, M.D., PH.D.¹

Departments of ¹Neurosurgery; ²Cancer Immunotherapy; ³Nuclear Medicine and Tracer Kinetics; ⁴Cancer Stem Cell Biology; ⁵Respiratory Medicine, Allergy, and Rheumatic Diseases; and ⁷Functional Diagnostic Science, Osaka University Graduate School of Medicine, Osaka; and ⁶Department of Biostatistics and Epidemiology, Yokohama City University Graduate School of Medicine, Yokohama, Japan

Object. Immunotherapy targeting the *Wilms tumor 1* (*WT1*) gene product is a promising treatment modality for patients with malignant gliomas, and there have been reports of encouraging results. It has become clear, however, that Gd-enhanced MR imaging does not reflect prognosis, thereby necessitating a more robust imaging evaluation system for monitoring response to WT1 immunotherapy. To meet this demand, the authors performed a voxel-wise parametric response map (PRM) analysis of ^{11}C -methionine PET (MET-PET) in WT1 immunotherapy and compared the data with the overall survival after initiation of WT1 immunotherapy (OS_{WT1}).

Methods. Fourteen patients with recurrent malignant glioma were included in the study, and OS_{WT1} was compared with: 1) volume and length change in the contrast area of the tumor on Gd-enhanced MR images; 2) change in maximum uptake of ^{11}C -methionine; and 3) a more detailed voxel-wise PRM analysis of MET-PET pre- and post-WT1 immunotherapy.

Results. The PRM analysis was able to identify the following 3 areas within the tumor core: 1) area with no change in ^{11}C -methionine uptake pre- and posttreatment; 2) area with increased ^{11}C -methionine uptake posttreatment (PRM^{MET}); and 3) area with decreased ^{11}C -methionine uptake posttreatment. While the results of Gd-enhanced MR imaging volumetric and conventional MET-PET analysis did not correlate with OS_{WT1} ($p = 0.270$ for Gd-enhanced MR imaging length, $p = 0.960$ for Gd-enhanced MR imaging volume, and $p = 0.110$ for MET-PET), the percentage of PRM^{MET} area showed excellent correlation ($p = 0.008$) with OS_{WT1} .

Conclusions. This study describes the limited value of Gd-enhanced MR imaging and highlights the potential of voxel-wise PRM analysis of MET-PET for monitoring treatment response in immunotherapy for malignant gliomas. Clinical trial registration no.: UMIN000002001.

(<http://thejns.org/doi/abs/10.3171/2011.12.JNS111255>)

KEY WORDS • glioma • ^{11}C -methionine PET • WT1 immunotherapy • parametric response map • oncology

MALIGNANT glioma remains a devastating intracranial neoplasm. In particular, patients with newly diagnosed GBM have a median overall survival of only 14.6 months, even when treated with chemotherapeutic agents such as temozolomide.¹⁷ On the other hand, the products of the *WT1* gene have been shown to be overexpressed in malignant gliomas,^{12,13} and this makes

Abbreviations used in this paper: GBM = glioblastoma multiforme; MET-PET = ^{11}C -methionine PET; OS_{WT1} = overall survival after initiation of Wilms tumor 1 immunotherapy; PRM = parametric response map; RECIST = Response Evaluation Criteria in Solid Tumors; ROI = region of interest; WT1 = Wilms tumor 1.

the WT1 antigen an attractive target for immunotherapy against malignant glioma.

The results of WT1 immunotherapy have been previously reported for the initial 21 patients participating in an ongoing Phase II clinical trial of WT1 vaccination for patients with recurrent malignant glioma, and the safety and efficacy of WT1 vaccination have been described (Phase I/II clinical trial of WT1 peptide-based vaccine for the patients with malignant tumors. UMIN000002001).⁹

This article contains some figures that are displayed in color online but in black and white in the print edition.

The median overall survival time after initiating WT1 immunotherapy was 36.7 weeks. In that report, the anti-tumor effect of the treatment was assessed by determining the response of the target lesions using MR imaging 12 weeks after initiating WT1 vaccination. The tumor length, corresponding to the contrast-enhanced area on Gd-enhanced MR images, was measured and analyzed according to RECIST version 1.0,¹⁸ with results reported as complete response, partial response, stable disease, and progressive disease.

In that analysis, however, the long-term survivors were assessed as having progressive disease at 12 weeks after WT1 vaccination initiation, suggesting that evaluation by contrast-enhanced T1-weighted MR imaging is not suitable for assessing the treatment response to WT1 immunotherapy. The fact that morphological imaging often does not adequately reflect the underlying tumor biology³ imposes a considerable demand to develop alternative biological markers for therapeutic response. Recently, a voxel-wise PRM has been developed to overcome the above-mentioned issue in other treatment modalities for malignant glioma.⁶⁻⁸

The present report focuses on the results in 14 patients who were enrolled in the same trial but were not included in the previous report. In this study, we have attempted to apply the voxel-wise PRM method to MET-PET in the setting of WT1 immunotherapy against recurrent malignant glioma and compare its clinical value with conventional analytical methods based on MR imaging and PET.

Methods

WT1 Immunotherapy

Patients received intradermal injections of 3.0 mg of modified 9-mer WT1 peptide emulsified with Montanide ISA51 adjuvant. The WT1 vaccinations were given weekly for 12 consecutive weeks. Twelve weeks after the initial vaccination, the response was evaluated by means of both MR imaging and MET-PET. Our local internal review board approved this treatment and written informed consent was obtained from all patients. Details of the procedures and protocol have been reported elsewhere.^{9,14}

Patient Selection

Between 2004 and 2010, 66 patients with recurrent malignant glioma were treated with WT1 immunotherapy as described above as part of an ongoing clinical trial (UMIN000002001). Nineteen of these 66 patients underwent evaluation by means of MET-PET. These patients were not included in our previous report.⁹ Five of these 19 patients—2 patients with intratumoral hematoma and 3 patients whose tumor volume was 2 cm³ or less as measured by MET-PET—were excluded from the current analysis. All 14 patients whose data were analyzed for this study underwent MR imaging and MET-PET before (pre-WT1) and 12 weeks after (post-WT1) WT1 vaccination. Detailed information pertaining to these 14 patients is listed in Table 1. The overall survival was measured from WT1 immunotherapy initiation, denoted as OS_{WT1}.

Magnetic Resonance Imaging

All MR images were obtained using a 3.0-T whole-body MR scanner (Signa, GE Medical Systems) with an acquisition time of approximately 3 minutes. After intravenous administration of Gd-diethylenetriamine penta-acetic acid (Gd-DTPA; 0.1 mmol/kg body weight), axial T1-weighted images were obtained using standard procedures. Those images were stored in 512 × 512 × 23 or 216 anisotropic voxels, with each voxel being 0.43 × 0.43 × 6.0 or 1.0 mm.

MET-PET Scans

All PET studies were performed using the Eminence PET system (Shimadzu Corp.). ¹¹C-methionine (111–222 MBq, 3–6 mCi), synthesized according to the method of Berger et al.,¹ was injected intravenously. Tracer accumulation was recorded over 15 minutes in 99 trans-axial slices from the entire brain. Total activity from 20 to 35 minutes after tracer injection was used for image reconstruction. The images were stored in 256 × 256 × 99 anisotropic voxels, with each voxel being 1 × 1 × 2.6 mm.

Tumor Length and Volume Measurement

Tumor length, corresponding to the contrast-enhanced area on T1-weighted MR images, was measured and analyzed according to RECIST version 1.0,¹⁸ using the ImageJ software from the National Institutes of Health (<http://rsb.info.nih.gov/ij/>).

Tumor volume was measured by performing a 3D threshold-based volume-of-interest analysis in all patients for contrast-enhanced lesions on Gd-enhanced MR images, using the ImageJ software. The contrast-enhanced area in each slice image was measured by manual tracking of the tumor boundaries, and the sum of the enhanced areas or high-uptake areas was multiplied by the slice interval.

Image Fusion and Registration

The MET-PET data were registered onto pre-WT1 contrast-enhanced T1-weighted standard anatomical images using normalized mutual information with the VINCI image analyzing software from the Max Planck Institute for Neurological Research in Cologne (<http://www.nf.mpg.de/vinci/>). Registration of the images was confirmed visually. The reported registration error for normalized mutual information is less than 1 mm.¹⁹ After image registration was completed, all image sets, including the standard anatomical MR images (pre-WT1) and MET-PET data (pre- and post-WT1), were converted into 256 × 256 × 256 isotropic, 1 × 1 × 1 mm images enabling further voxel-wise analysis of the images (Fig. 1).

Data Processing and ROI Selection

Three data sets (standard anatomical images and MET-PET data) were exported to in-house software written in MATLAB 7.6 (MathWorks) for further analysis. Regions of interest were selected as follows: for normal brain tissue, the contralateral hemisphere of the tumor was selected, including both the gray and white matter; for tumor, contrast-enhanced lesions were selected.

PET monitoring of immunotherapy response

TABLE 1: Summary of clinical and demographic characteristics of 14 patients*

Case No.	Age (yrs),† Sex	ECOG PS	Diagnosis	Response per RECIST	OS _{WT1} (wks)‡	Tumor Vol by MET-PET (cm ³)§
1	43, M	2	GBM	SD	87.1	31.2
2	64, M	1	GBM	PD	144.7	63.8
3	76, M	1	GBM	SD	144.6	29
4	60, F	0	GBM	SD	61.7	58.1
5	20, F	0	GBM	PR	29.3	24.9
6	64, F	1	AA	SD	65.0	51
7	29, M	2	GBM	PD	20.9	15.4
8	28, M	1	GBM	SD	57.7	9
9¶	62, M	0	gliosarcoma	SD	77.0	11.5
10	36, F	1	AA	SD	60.3	3.8
11	44, M	0	GBM	PD	48.1	13.2
12	62, F	1	GBM	PD	18.7	5
13	51, M	0	GBM	PD	35.0	39.3
14	39, F	1	GBM	PD	27.6	15.2

* AA = anaplastic astrocytoma; ECOG PS = Eastern Cooperative Oncology Group Performance Status; PD = progressive disease; PR = partial response; SD = stable disease.

† Mean 48.4 years.

‡ Median 59.0 weeks.

§ Median 26.5 cm³.

¶ The patient in Case 9 was alive as of this writing.

Parametric Response Map Calculation Algorithm

As in Fig. 1, post-WT1 ¹¹C-methionine uptake was plotted as a function of pre-WT1 ¹¹C-methionine uptake in both normal brain and Gd-enhancing lesions. A linear regression fitting was applied to the data obtained by the ROI placed at the normal brain (Fig. 1, blue line), which can be expressed as follows: post-WT1 MET-PET = pre-WT1 MET-PET, where “post-WT1 MET-PET” and “pre-WT1 MET-PET” are the tumor/normal tissue (T/N) ratio of pre- and post-WT1 ¹¹C-methionine PET.

Next, the magnitude of deviation of each data point (*i*) from the expected linear regression fitting was calculated as follows:

$$\text{deviation}_i = [(\text{post-WT1 MET-PET})_i - (\text{pre-WT1 MET-PET})_i] / \sqrt{2}$$

The parametric response map (PRM) of each data point was defined as follows:

$$\text{PRM}_i = \text{deviation}_i - \mu / \rho$$

where μ and ρ are the mean and standard deviation of deviation_{*i*} within the ROI placed at the normal brain. In other words, PRM is identical to the z-score of each data point in the lesion from the expected linear regression line calculated for normal brain.

Statistical Analysis

Statistical analyses were carried out using a Kaplan-Meier survival analysis with the log-rank test if not specified otherwise. A *p* value < 0.05 was considered statistically significant, and all statistical computation was performed using Prism 5 (GraphPad Software, Inc.) or JMP 9.0 (SAS Institute, Inc.).

Results

Applying the PRM Calculation to WT1 Immunotherapy Patients

The PRM calculation, described above and in Fig. 1, was successfully performed in all 14 cases. The actual process that was performed is described below by presenting 2 representative cases, one (Case 2) in which the patient had a relatively long OS_{WT1} of 144.7 weeks and was considered a treatment responder, and another (Case 7) in which the patient had a relatively short OS_{WT1} of 20.9 weeks and was considered a treatment nonresponder.

Representative Treatment Responder. A representative case involving a treatment responder (Case 2) is illustrated in Fig. 2. First, a voxel-wise analysis was performed in normal brain tissue (Figs. 1 and 2). As shown in Fig. 2, pre- and post-WT1 ¹¹C-methionine uptake showed good positive linear correlation in normal brain tissue. A linear regression line and the ± 2 SD distribution range were calculated. Subsequently, the same analysis was performed in a tumor lesion. A contrast-enhanced area was selected as the ROI for analysis. In this particular case, most voxels were distributed in the -2 SD area, suggesting that ¹¹C-methionine uptake decreased after WT1 immunotherapy (Fig. 2). This area is presented as PRM^{-MET} (PRM with reduced methionine uptake).

This patient survived for 144.7 weeks after initiation of WT1 immunotherapy, although the contrast-enhanced area increased after WT1 immunotherapy, categorizing this patient as having progressive disease in the Gd-enhanced MR imaging-based RECIST analysis.

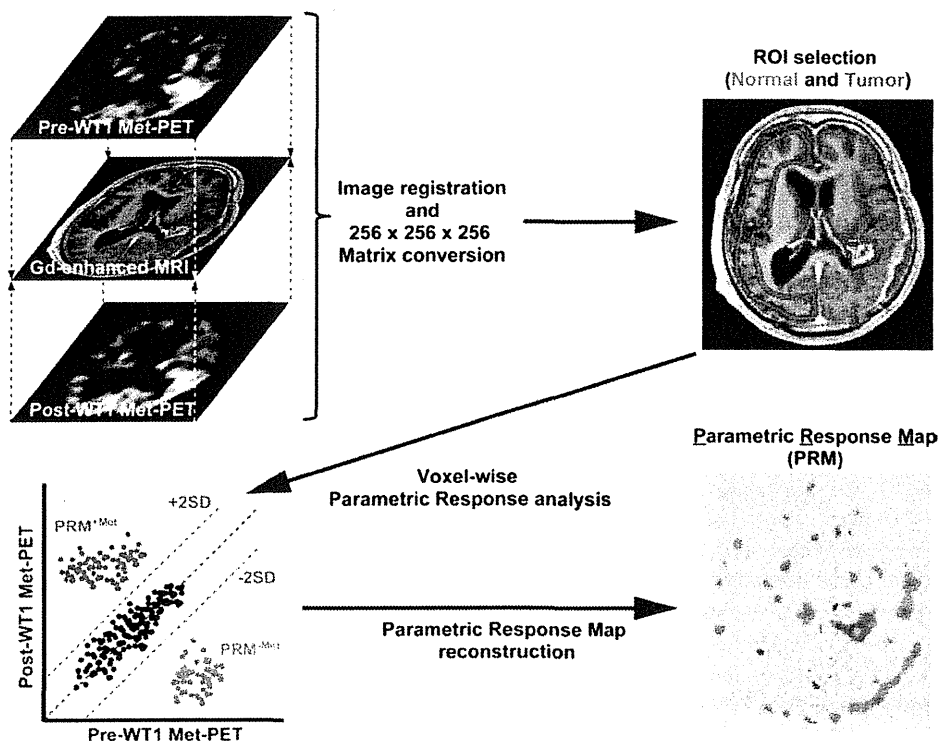


Fig. 1. Image processing procedures. ^{11}C -methionine PET data obtained before and 12 weeks after WT1 immunotherapy initiation were fused and registered onto conventional contrast-enhanced MR images. All 3 images were converted into a $256 \times 256 \times 256$, 1-mm isotropic image matrix. Post-WT1 ^{11}C -methionine uptake was plotted as a function of pre-WT1 ^{11}C -methionine uptake. After calculating the linear regression line with the ± 2 SD distribution range in contralateral normal brain tissue, an ROI was set at the contrast-enhanced pre-WT1 immunotherapy lesion. The obtained plots were categorized into the following 3 areas: 1) area of no change in ^{11}C -methionine uptake pre- and posttreatment, 2) area with increased ^{11}C -methionine uptake posttreatment (PRM^{+MET}), and 3) area with decreased ^{11}C -methionine uptake posttreatment (PRM^{-MET}). These areas were reconstructed in images for visual inspection (PRM^{+MET} in red and PRM^{-MET} in blue).

Representative Treatment Nonresponder. A representative case in which the patient had only a short OS_{WT1} (Case 7) is illustrated in Fig. 3. The same analysis as described above was performed. In this particular case, most voxels were distributed in the +2 SD area (PRM with increased methionine uptake [PRM^{+MET}]), suggesting that ^{11}C -methionine uptake increased after WT1 immunotherapy. This patient survived for 20.9 weeks after initiation of WT1 immunotherapy.

Correlation of Treatment Response Assessment and OS_{WT1}

Magnetic Resonance Imaging–Based Assessment. To assess the validity of evaluating the response to WT1 immunotherapy using contrast-enhanced MR imaging, the changes in length and volume of the tumor before and 12 weeks after initiating WT1 immunotherapy were calculated. As in Fig. 4A and B, both methods using Gd-enhanced MR imaging failed to show positive correlation with OS_{WT1} ($p = 0.270$ and 0.960 , respectively).

Conventional MET-PET Analysis. To assess the validity of evaluating the response to WT1 immunotherapy using MET-PET, the changes in maximum ^{11}C -methionine uptake assessed using the tumor/normal tissue ratio (T/N

max) before and 12 weeks after initiating WT1 immunotherapy were calculated. Change of T/N max failed to show any statistically significant correlation with OS_{WT1} ($p = 0.110$) (Fig. 4C).

Parametric Response Map Analysis. Finally, correlation of the proposed voxel-wise PRM of MET-PET with OS_{WT1} was investigated. Each voxel of contrast-enhanced area on the pretreatment MR images was categorized as a no-change area, PRM^{+MET}, or PRM^{-MET}, according to no change, increase, or decrease, respectively, in methionine uptake 12 weeks after initiation of WT1 immunotherapy. The percentage of the 3 categories was calculated 3-dimensionally and correlated with OS_{WT1} (Fig. 5). While the percentage of the PRM^{-MET} area showed moderate correlation with OS_{WT1} ($p = 0.100$) (Fig. 5 left), the percentage of the PRM^{+MET} area showed excellent correlation with OS_{WT1} ($p = 0.008$) (Fig. 5 right). A threshold of 5% for PRM^{+MET} yielded the best performance for discriminating WT1 immunotherapy responders from nonresponders (Fig. 5 right). When a Cox proportional hazard model was applied, adjusted by age (cutoff 50 years of age) and performance status (0 or 1 and 2), a threshold of 5% for PRM^{+MET} still remained as the only statistically significant factor ($p = 0.01$).

PET monitoring of immunotherapy response

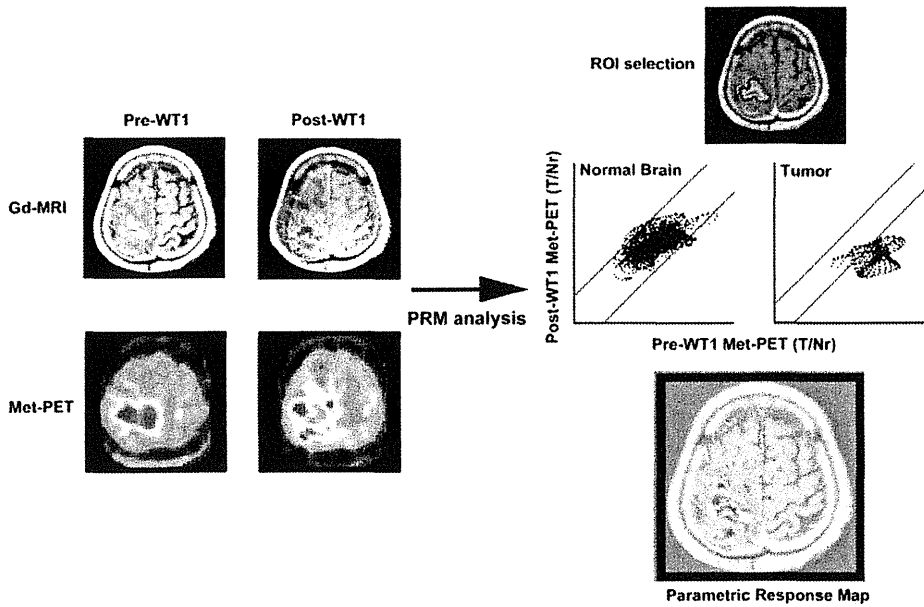


Fig. 2. Case 2. A representative treatment responder with recurrent GBM (OS_{WT1} 144.7 weeks). Images were analyzed as in Fig. 1. Voxel-wise PRM analysis revealed that most of the contrast-enhanced lesion was within the PRM^{-MET} area. Although the OS_{WT1} was 144.7 weeks, conventional MR imaging evaluated the response as progressive disease. Gd-MRI = Gd-enhanced MR imaging; T/Nr = T/N max.

Discussion

Conventionally, MR imaging is used to evaluate response to treatment in glioma patients. The maximum length of the contrast-enhanced area is measured and the effect of treatment is analyzed according to RECIST. This method is based on previous reports showing RE-

CIST to be useful in determining objective responses of contrast-enhancing brain tumors to therapy. Moreover, those reports showed that use of RECIST was comparable to volumetric methods.^{5,16} On the other hand, problems with using MR imaging-based tumor measurement as an indicator of treatment response have been reported. For example, temozolomide-based chemoradiotherapy for

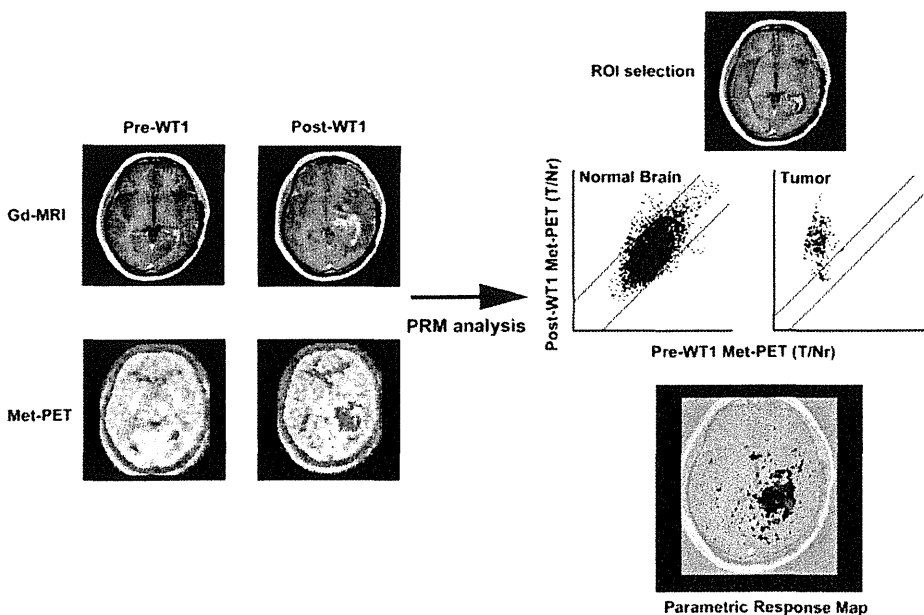


Fig. 3. Case 7. A representative treatment nonresponder with recurrent GBM (OS_{WT1} 20.9 weeks). Images were analyzed as in Fig. 1. Voxel-wise PRM analysis revealed that most of the contrast-enhanced lesion was within the PRM^{+MET} area, suggesting that the patient was not responsive to WT1 immunotherapy.

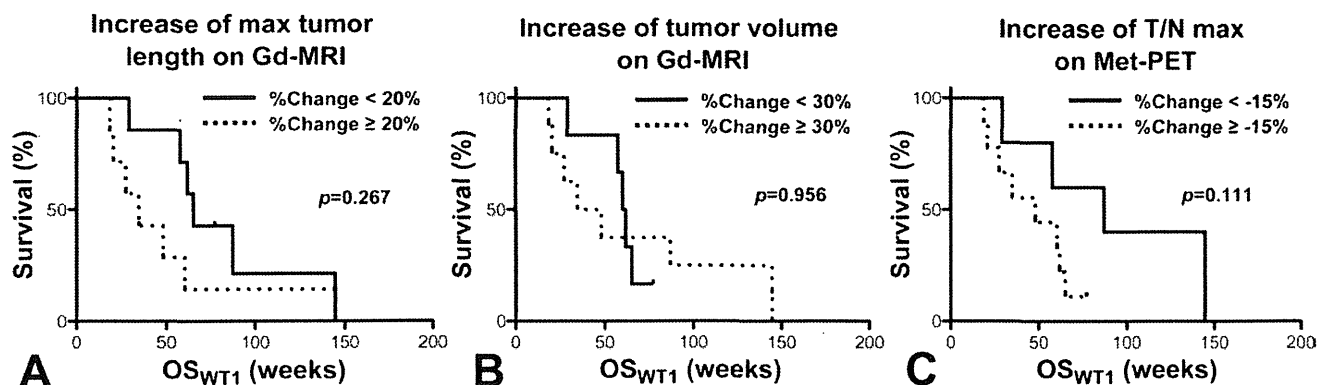


FIG. 4. Correlation of OS_{WT1} with changes in tumor length and volume using contrast-enhanced MR imaging and the T/N max of MET-PET. Correlations between OS_{WT1} and changes (from before WT1 immunotherapy to 12 weeks after immunotherapy initiation) on Gd-enhanced MR imaging—measured tumor length (A), volume (B), and T/N max of MET-PET (C) are presented. The correlations were not statistically significant ($p = 0.270, 0.960, \text{ and } 0.110$, respectively; 14 cases).

newly diagnosed GBM results in a transient increase in tumor enhancement on MR imaging in 20%–30% of patients (pseudoprogression), which is difficult to differentiate from true tumor progression.² Similarly, in the present study, changes in tumor length and volume measured by contrast-enhanced MR imaging after WT1 immunotherapy did not correlate with OS_{WT1} (Fig. 4), suggesting that contrast-enhanced MR imaging is inappropriate for evaluating the clinical outcome of WT1 immunotherapy. Unlike chemotherapy or radiotherapy, immunotherapy causes an inflammatory reaction in the tumor, which results in infiltration of inflammatory cells, dilation of capillary vessels, and increased capillary permeability. Thus, it is possible that contrast enhancement does not reflect the tumor activity but rather represents the immune reaction in situ.

On the other hand, MET-PET provides high-resolution metabolic information about the tumor in vivo,¹⁰ information that is impossible to obtain using MR imaging. Previous studies have shown that the ratio of the maximum ¹¹C-methionine uptake in tumor compared with the contralateral normal brain (T/N max) reflects prognos-

is.^{4,11} However, gliomas are heterogeneous in nature and have heterogeneous uptake of ¹¹C-methionine. In fact, we have previously demonstrated that ¹¹C-methionine uptake correlates with tumor cell density by comparing MET-PET images with stereotactically sampled tissue.¹⁵ Thus, instead of analyzing T/N max, which could result in comparisons between different locations within the tumor, a better method is to analyze the change in ¹¹C-methionine uptake in each anatomical location to elucidate the global change in ¹¹C-methionine uptake within the tumor. To satisfy this need, a voxel-wise PRM analysis^{6–8} was used in the present study and produced excellent correlation between OS_{WT1} and the percentage of PRM^{+MET} (Fig. 5). This method showed far better correlation with OS_{WT1} than changes in T/N max by MET-PET, suggesting that the voxel-wise PRM is the most suitable method for assessing the treatment response of gliomas. Moreover, although the number of cases analyzed was small, a threshold of 5% for PRM^{+MET} was the best indicator for discriminating WT1 immunotherapy responders from nonresponders in terms of survival time (Fig. 5 right). A similar method has already been applied for diffusion or perfusion MR im-

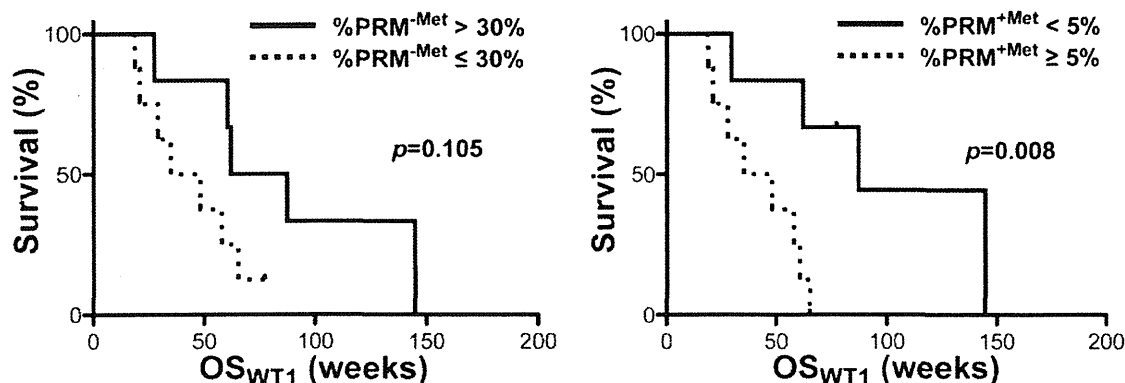


FIG. 5. Correlation of OS_{WT1} with PRM^{-MET} and PRM^{+MET}. Correlations between OS_{WT1} and percentage areas of PRM^{-MET} (left) and PRM^{+MET} (right) are presented. The percentage of PRM^{-MET} within the contrast-enhanced lesion before WT1 immunotherapy initiation correlated best with OS_{WT1} ($p = 0.008$; 14 cases).

PET monitoring of immunotherapy response

aging analysis in glioma treatment using temozolomide and radiation therapy and has been suggested as an early biomarker for treatment response.⁶⁻⁸ The main difference between voxel-wise PRM analysis and conventional imaging analysis is that voxel-wise PRM analysis allows us to identify the location and extent of areas that responded to therapy, rather than comparing the maximum values of the pre- and posttreatment evaluation modality, which could be comparing different locations.

There are, however, limitations that should be noted. Because pre- and posttreatment ¹¹C-methionine uptake is registered and compared, this method cannot be used when the shape or size dramatically change during therapy due to cyst formation or intratumoral hemorrhage. A more advanced method that could correct for tissue deformation is required to compensate for these changes. As the images compared were obtained 12 weeks apart, it is necessary to investigate the possibility of comparing images obtained in shorter intervals. Another limitation of this study is the retrospective nature of the data analysis and the limited sample size. Although a 5% cutoff of PRM^{+MET} yields the best result for the survival analysis, a prospective study with a much larger sample size will be necessary to obtain the most suitable cutoff value. Moreover, other modalities, such as perfusion or diffusion MR images should also be investigated in a similar manner to elucidate whether these modalities could also be used for evaluating immunotherapy for malignant gliomas.

Conclusions

We performed a voxel-wise PRM analysis of MET-PET before and 12 weeks after WT1 immunotherapy initiation to evaluate the clinical responses to WT1 immunotherapy in recurrent malignant glioma patients. This method holds promise for evaluating the dynamics of immunotherapy, which can be difficult to assess using conventional Gd-enhanced MR imaging.

Disclosure

The authors report no conflict of interest concerning the materials or methods used in this study or the findings specified in this paper. This work was supported in part by grants to Dr. Kinoshita from the Osaka Cancer Research Foundation, the Konica Minolta Imaging Science Foundation, the Osaka Cancer Researcher Training Fund, the Takeda Science Foundation, the Sagawa Foundation for Promotion of Cancer Research, and the Ministry of Education, Science and Culture of Japan, and by grants to Drs. Chiba and Hashimoto from the Ministry of Education, Science and Culture of Japan.

Author contributions to the study and manuscript preparation include the following. Conception and design: Kinoshita, Chiba, Tsuboi, Hashimoto, Yoshimine. Acquisition of data: Kinoshita, Chiba, Okita, Tsuboi, Isohashi, Kagawa, Fujimoto, Oji, Oka, Shimosegawa, Hatazawa, Hashimoto, Yoshimine. Analysis and interpretation of data: all authors. Drafting the article: Kinoshita, Chiba, Okita, Morita, Hashimoto, Yoshimine. Critically revising the article: all authors. Reviewed submitted version of manuscript: all authors. Approved the final version of the manuscript on behalf of all authors: Kinoshita. Statistical analysis: Kinoshita. Administrative/technical/material support: Tsuboi, Hashimoto, Yoshimine. Study supervision: Tsuboi, Oji, Oka, Hatazawa, Hashimoto, Yoshimine.

Acknowledgment

The authors thank Ms. Mariko Kakinoki (Department of Neurosurgery, Osaka University Graduate School of Medicine) for her assistance in the preparation of this manuscript.

References

- Berger G, Maziere M, Knipper R, Prenant C, Comar D: Automated synthesis of ¹¹C-labelled radiopharmaceuticals: imipramine, chlorpromazine, nicotine and methionine. *Int J Appl Radiat Isot* **30**:393-399, 1979
- Brandsma D, Stalpers L, Taal W, Sminia P, van den Bent MJ: Clinical features, mechanisms, and management of pseudo-progression in malignant gliomas. *Lancet Oncol* **9**:453-461, 2008
- Brasch R, Pham C, Shames D, Roberts T, van Dijke K, van Bruggen N, et al: Assessing tumor angiogenesis using macro-molecular MR imaging contrast media. *J Magn Reson Imaging* **7**:68-74, 1997
- De Witte O, Goldberg I, Wikler D, Rorive S, Damhaut P, Monclus M, et al: Positron emission tomography with injection of methionine as a prognostic factor in glioma. *J Neurosurg* **95**:746-750, 2001
- Galanis E, Buckner JC, Maurer MJ, Sykora R, Castillo R, Ballman KV, et al: Validation of neuroradiologic response assessment in gliomas: measurement by RECIST, two-dimensional, computer-assisted tumor area, and computer-assisted tumor volume methods. *Neuro Oncol* **8**:156-165, 2006
- Galbán CJ, Chenevert TL, Meyer CR, Tsien C, Lawrence TS, Hamstra DA, et al: The parametric response map is an imaging biomarker for early cancer treatment outcome. *Nat Med* **15**:572-576, 2009
- Galbán CJ, Chenevert TL, Meyer CR, Tsien C, Lawrence TS, Hamstra DA, et al: Prospective analysis of parametric response map-derived MRI biomarkers: identification of early and distinct glioma response patterns not predicted by standard radiographic assessment. *Clin Cancer Res* **17**:4745-4760, 2011
- Hamstra DA, Chenevert TL, Moffat BA, Johnson TD, Meyer CR, Mukherji SK, et al: Evaluation of the functional diffusion map as an early biomarker of time-to-progression and overall survival in high-grade glioma. *Proc Natl Acad Sci U S A* **102**:16759-16764, 2005
- Izumoto S, Tsuboi A, Oka Y, Suzuki T, Hashiba T, Kagawa N, et al: Phase II clinical trial of Wilms tumor 1 peptide vaccination for patients with recurrent glioblastoma multiforme. *J Neurosurg* **108**:963-971, 2008
- Jager PL, Vaalburg W, Pruijm J, de Vries EG, Langen KJ, Piers DA: Radiolabeled amino acids: basic aspects and clinical applications in oncology. *J Nucl Med* **42**:432-445, 2001
- Nariai T, Tanaka Y, Wakimoto H, Aoyagi M, Tamaki M, Ishiwata K, et al: Usefulness of L-[methyl-¹¹C] methionine-positron emission tomography as a biological monitoring tool in the treatment of glioma. *J Neurosurg* **103**:498-507, 2005
- Oji Y, Ogawa H, Tamaki H, Oka Y, Tsuboi A, Kim EH, et al: Expression of the Wilms' tumor gene WT1 in solid tumors and its involvement in tumor cell growth. *Jpn J Cancer Res* **90**:194-204, 1999
- Oji Y, Suzuki T, Nakano Y, Maruno M, Nakatsuka S, Jomgeow T, et al: Overexpression of the Wilms' tumor gene WT1 in primary astrocytic tumors. *Cancer Sci* **95**:822-827, 2004
- Oka Y, Tsuboi A, Taguchi T, Osaki T, Kyo T, Nakajima H, et al: Induction of WT1 (Wilms' tumor gene)-specific cytotoxic T lymphocytes by WT1 peptide vaccine and the resultant cancer regression. *Proc Natl Acad Sci U S A* **101**:13885-13890, 2004
- Okita Y, Kinoshita M, Goto T, Kagawa N, Kishima H, Shi-

- mosegawa E, et al: (11)C-methionine uptake correlates with tumor cell density rather than with microvessel density in glioma: a stereotactic image-histology comparison. **Neuroimage** **49**:2977–2982, 2010
16. Shah GD, Kesari S, Xu R, Batchelor TT, O'Neill AM, Hochberg FH, et al: Comparison of linear and volumetric criteria in assessing tumor response in adult high-grade gliomas. **Neuro Oncol** **8**:38–46, 2006
17. Stupp R, Mason WP, van den Bent MJ, Weller M, Fisher B, Taphoorn MJ, et al: Radiotherapy plus concomitant and adjuvant temozolomide for glioblastoma. **N Engl J Med** **352**:987–996, 2005
18. Therasse P, Arbuck SG, Eisenhauer EA, Wanders J, Kaplan RS, Rubinstein L, et al: New guidelines to evaluate the response to treatment in solid tumors. European Organization for Research and Treatment of Cancer, National Cancer Institute of the United States, National Cancer Institute of Canada. **J Natl Cancer Inst** **92**:205–216, 2000
19. Veninga T, Huisman H, van der Maazen RW, Huizenga H: Clinical validation of the normalized mutual information method for registration of CT and MR images in radiotherapy of brain tumors. **J Appl Clin Med Phys** **5**:66–79, 2004

Manuscript submitted July 22, 2011.

Accepted December 8, 2011.

Please include this information when citing this paper: published online January 13, 2012; DOI: 10.3171/2011.12.JNS111255.

Address correspondence to: Manabu Kinoshita, M.D., Ph.D., Department of Neurosurgery, Osaka University Graduate School of Medicine, 2-2 Yamadaoka, Suita, Osaka 565-0871, Japan. email: m-kinoshita@nsurg.med.osaka-u.ac.jp.

Long-term outcomes of intraluminal brachytherapy in combination with external beam radiotherapy for superficial esophageal cancer

Yuji Murakami · Yasushi Nagata · Ikuno Nishibuchi · Tomoki Kimura · Masahiro Kenjo · Yuko Kaneyasu · Tomoyuki Okabe · Yasutoshi Hashimoto · Yukio Akagi

Received: 23 February 2011 / Accepted: 24 June 2011 / Published online: 12 July 2011
© Japan Society of Clinical Oncology 2011

Abstract

Background The aim of this study was to assess the long-term outcomes of combining high-dose-rate intraluminal brachytherapy (IBT) with external beam radiotherapy (EBRT) for superficial esophageal cancer (SEC).

Methods From 1992 to 2002, 87 patients with T1N0M0 thoracic esophageal cancer received IBT in combination with EBRT. Of these, 44 had mucosal cancer and 43 had submucosal cancer. For patients with tumor invasion within the lamina propria mucosa, IBT alone was performed ($n = 27$). IBT boost following EBRT was performed for patients with tumor invasion in the muscularis mucosa or deeper ($n = 60$). No patient received chemotherapy.

Results The median follow-up time was 94 months. For mucosal cancer, the 5-year locoregional control (LRC), cause-specific survival (CSS) and overall survival (OS) rates were 75, 97 and 84%, respectively, and 49, 55 and 31%, respectively, for submucosal cancer. Tumor depth

was a significant factor associated with LRC ($p = 0.02$), CSS ($p < 0.001$) and OS ($p < 0.001$) by univariate analysis. Multivariate analysis revealed that tumor depth was the only significant predictor for OS ($p = 0.003$). Late toxicities of grade 3 or higher in esophagus, pneumonitis, pleural effusion and pericardial effusion were observed in 5, 0, 0 and 1 patients, respectively. Grade ≥ 3 events of cardiac ischemia and heart failure after radiotherapy were observed in 9 patients, and history of heart disease before radiotherapy was the only significant factor ($p = 0.002$).

Conclusion There was a clear difference in outcomes of IBT combined with EBRT between mucosal and submucosal esophageal cancers. More intensive treatment should be considered for submucosal cancer.

Keywords Esophageal cancer · Superficial esophageal cancer · Squamous cell carcinoma · Radiotherapy · Brachytherapy

Y. Murakami (✉) · Y. Nagata · I. Nishibuchi · T. Kimura · M. Kenjo · Y. Kaneyasu
Department of Radiation Oncology, Hiroshima University Graduate School of Biomedical Sciences, 1-2-3 Kasumi, Minami-ku, Hiroshima 734-8551, Japan
e-mail: yujimura@hiroshima-u.ac.jp

Y. Nagata
e-mail: nagat@hiroshima-u.ac.jp

I. Nishibuchi
e-mail: ikuno@hiroshima-u.ac.jp

T. Kimura
e-mail: tkimura@hiroshima-u.ac.jp

M. Kenjo
e-mail: kenjom@hiroshima-u.ac.jp

Y. Kaneyasu
e-mail: kaneyasu@hiroshima-u.ac.jp

T. Okabe
Department of Radiology, Hiroshima City Hospital, 7-33 Motomachi, Naka-ku, Hiroshima 730-8518, Japan
e-mail: t-okabe@pd6.so-net.ne.jp

Y. Hashimoto
Department of Radiology, Chugoku Rosai General Hospital, 1-5-1 Tagaya, Kure, Hiroshima 737-0193, Japan
e-mail: yasu06340829@yahoo.co.jp

Y. Akagi
Hiroshima Heiwa Clinic, 1-21 Kawaramachi, Naka-ku, Hiroshima 730-0856, Japan
e-mail: akagi@aoikai.jp

Introduction

Advances in endoscopic equipment have enabled the treatment of increasing numbers of patients with superficial esophageal cancer (SEC) [1–3], which can be divided into mucosal and submucosal cancers. In SEC patients treated by surgery, pathological analyses have shown significant differences in rates of lymph node (LN) metastasis according to tumor depth: 0–6% in the mucosa and 38–53% in the submucosa [4–9]. Among mucosal cancer patients, when tumor cells were found within the lamina propria mucosa there was almost no LN metastasis (0–1.4%), whereas in patients with tumors invading to the muscularis mucosa, a ratio of LN metastases of more than 10% was reported [4]. Endoscopic resection is generally indicated for patients with tumors invading within the lamina propria mucosa. For patients with tumors invading the muscularis mucosa or deeper, esophagectomy with systematic LN dissection is the main treatment. However, due to the extent of surgery, the alternative of radiotherapy (RT) is often selected for patients in poor medical condition or advanced age, and its efficacy has been reported by several authors [10–14].

Brachytherapy is a RT technique that can deliver a high dose to local tumors while sparing exposure to the surrounding normal tissues. Intraluminal brachytherapy (IBT) has been used mainly for SEC in Japan, while in Western countries IBT has been used with palliative intent for malignant esophageal strictures. The efficacy of IBT combined with external beam radiotherapy (EBRT) for SEC has been reported [15–19], and this method was considered an effective treatment in Japan in the 1990s. We performed IBT combined with EBRT for SEC patients until 2002, following the introduction in 1991 of the high-dose-rate iridium-192 remote afterloading system (micro-Selectron HDR from Nucletron, Netherlands). Subsequently, the protocol was changed and chemoradiotherapy (CRT) was introduced for SEC. In this study, the long-term outcomes of IBT combined with EBRT for SEC were evaluated.

Patients and methods

Patient and tumor characteristics

Patient and tumor characteristics are listed in Table 1. There were 87 patients eligible for this study with T1N0M0 (International Union Against Cancer TNM system, 1997) thoracic esophageal cancer who received IBT combined with EBRT between 1992 and 2002. The median age was 70 years (range 43–89), with 80 males and 7 females. Sixty-nine patients had Karnofsky performance status

Table 1 Patient and tumor characteristics

Characteristics	No. of patients (%)
Age (years)	
Range	43–89
Median	70
Gender	
Male	80 (92)
Female	7 (8)
KPS	
90–100	69 (79)
60–80	18 (21)
Reasons for selecting RT	
Medically inoperable	54 (62)
Patient refused surgery	33 (38)
Double cancer	
All	28 (32)
Within 5 years	16 (18)
Histology	
Squamous cell	86 (99)
Adenocarcinoma	1 (1)
Tumor sites	
Upper thoracic	8 (9)
Middle thoracic	65 (75)
Lower thoracic	14 (16)
Tumor depth	
Mucosal	44 (51)
Submucosal	43 (49)

KPS Karnofsky performance status, RT radiotherapy

(KPS) of 90 or more. RT was selected in 54 patients who were judged medically inoperable and in 33 patients who declined surgery. Medically inoperable factors included concurrent illnesses, advanced age and coexisting malignancies. Main concurrent illnesses included heart disease in 14, hepatic disease in 18 and pulmonary disease in 9. Coexisting malignancies were observed in 28 patients, and 16 had malignancies within 5 years before the diagnosis of esophageal cancer. Among them, 12 had active malignancies. Taken together, these malignancies were distributed as follows: gastric cancer in 11, head and neck cancer in 10, hepatocellular carcinoma in 4, colorectal cancer in 3 and lung cancer in 2. Histologically, 86 patients had squamous cell carcinoma and one had adenocarcinoma. Tumor sites were upper thoracic in 8 patients, middle thoracic in 65 and lower thoracic in 14. Forty-four had mucosal cancer and 43 had submucosal cancer. Of the 44 mucosal cancer patients, 25 received incomplete endoscopic mucosal resection (EMR) for tumors within the lamina propria mucosa, i.e., positive margin or partial resection of multiple or large lesions for the purpose of diagnosing tumor depth.

Treatment

Intraluminal brachytherapy was performed using the high-dose-rate iridium-192 remote afterloading system. The double-balloon applicator was used for IBT. The outer diameter of the applicator was either 16 or 20 mm, and the latter was mainly used. A prescribed dose was calculated at a depth of 5 mm from the surface of the esophageal mucosa.

EBRT was administered with 6 or 18 MV X-rays. After irradiation with 45–46 Gy using a fractional dose of 1.8–2.0 Gy to the primary tumor and regional LN area with anterior–posterior opposed beams, a planned dose was delivered to the primary tumor with oblique opposed beams to spare the spinal cord.

For patients with tumors within the lamina propria mucosa who had almost no risk of LN metastases, IBT alone was performed ($n = 27$). IBT was performed 5 days per week and irradiation doses were 35 Gy/14 fractions in 15 patients, 36 Gy/18 fractions in 9, 30 Gy/15 fractions in 2 and 25 Gy/5 fractions in 1.

Intraluminal brachytherapy boost following EBRT was performed for patients with tumors in the muscularis mucosa or deeper who had risk of LN metastases ($n = 60$). Irradiation doses of EBRT were 50–58 Gy/25–29 fractions (median 54 Gy) in cases of tumors in the muscularis mucosa or inner one-third of the submucosa and 54–61 Gy/27–33 fractions (median 60 Gy) in cases of tumors in the outer two-thirds of the submucosa. The IBT boost was generally performed immediately after EBRT using a schedule of 5 days per week. IBT boost doses were 10 Gy/4 fractions in 29, 10 Gy/5 fractions in 25, 10 Gy/2 fractions in 3, 7.5 Gy/3 fractions in 1, and 15 Gy/3 fractions in 1.

In this study, no patient received chemotherapy.

Analysis

The data were updated in June 2009. The median follow-up time for survivors was 94 months (range 28–187) and for all patients 64 months (range 2–187). There were 3 patients who were lost to follow-up within 60 months from RT. The follow-up periods of these 3 patients were 28, 56 and 57 months. Complete response (CR) was defined as the disappearance of the primary tumor by endoscopic biopsy. Overall survival (OS) was defined as the time from the initiation of RT to death from any cause. Cause-specific survival (CSS) was defined as the time from the initiation of RT to death due to esophageal cancer. Locoregional control (LRC) was calculated from the initiation of RT to the earliest events of recurrences in esophageal primary site, esophageal metachronous cancers and regional LN metastases. OS, CSS and LRC rates were calculated using the Kaplan–Meier method. Comparison of data was analyzed by Fisher's exact test. Univariate (UVA) and multivariate analyses (MVA) were performed using the log-rank test and the Cox proportional hazards test. A p value of <0.05 was considered significant. Toxicities were assessed using the Common Terminology Criteria for Adverse Events (CTCAE) v3.0.

Results

Response and failures

Treatment outcomes are shown in Table 2. Initial response was evaluated 8–181 days (median 31 days) after RT. Two patients were not evaluated because one died in a traffic accident soon after treatment, and concurrent illness

Table 2 Treatment outcomes

Outcomes	No. of patients (%)		
	Mucosal ($n = 44$)	Submucosal ($n = 41$)	Total ($n = 85$)
Initial response (evaluable cases)			
Complete response	43 (98)	40 (98)	83 (98)
Partial response	1 (2)	1 (2)	2 (2)
Recurrences			
Locoregional	14 (32)	19 (46)	30 (39)
Esophagus—primary site	5 (11)	8 (20)	13 (15)
Esophagus—metachronous	8 (18)	4 (10)	12 (14)
Lymph node—in EBRT field	0 (0)	1 (2)	1 (1)
Lymph node—out of EBRT field	1 (2)	4 (10)	5 (6)
Distant	0 (0)	1 (2)	1 (1)
Unknown	1 (2)	1 (2)	2 (2)

EBRT external beam radiotherapy, RT radiotherapy